BIANCA, a biophysical model of cell survival and chromosome damage by protons, C-ions and He-ions at energies and doses used in hadrontherapy

To cite this article before publication: Mario Pietro Carante *et al* 2018 *Phys. Med. Biol.* in press https://doi.org/10.1088/1361-6560/aab45f

BIANCA, a biophysical model of cell survival and chromosome damage by protons, C-ions and He-ions at energies and doses used in hadrontherapy

Mario Pietro Carante[1,2], Chiara Aimè[1], John James Tello Cajiao[1,2,3] and Francesca Ballarini[1,2]

[1] *University of Pavia, Physics Department, via Bassi 6, I-27100 Pavia, Italy*
[2] *INFN-Sezione di Pavia, via Bassi 6, I-27100 Pavia, Italy*
[3] *Universidade Estadual de Campinas, Cidade Universitária Zeferino Vaz. Campinas, SP, Brazil*

E-mail addresses

M. P. Carante: mario.carante@pv.infn.it

C. Aimè: chiara.aime01@universitadipavia.it

J. J. Tello: fisk2190@gmail.com

F. Ballarini: francesca.ballarini@unipv.it

Corresponding author: Francesca Ballarini

University of Pavia

Physics Department

Via Bassi 6, I-27100 Pavia, Italy

Tel. ++39 0382 987949

e-mail: francesca.ballarini@unipv.it

Abstract

An upgraded version of the BIANCA II biophysical model, which describes more realistically interphase chromosome organization and the link between chromosome aberrations and cell death, was applied to V79 and AG01522 cells exposed to protons, C-ions and He-ions over a wide LET interval (0.6-502 keV/μm), as well as proton-irradiated U87 cells . The model assumes that i) ionizing radiation induces DNA "Cluster Lesions" (CLs), where by definition each CL produces two independent chromosome fragments; ii) fragment (distance-dependent) mis-rejoining, or un-rejoining, produces chromosome aberrations; iii) some aberrations lead to cell death. The CL yield, which mainly depends on radiation quality but is also modulated by the target cell, is an adjustable parameter. The fragment un-rejoining probability, *f*, is the second, and last, parameter. The value of *f*, which is assumed to depend on the cell type but not on radiation quality, was taken from previous studies, and only the CL yield was adjusted in the present work.

Good agreement between simulations and experimental data was obtained, suggesting that BIANCA II is suitable for calculating the biological effectiveness of hadrontherapy beams. For both V79 and AG01522 cells, the mean number of CLs per micrometer was found to increase with LET in a linear-quadratic fashion before the over-killing region, where a less rapid increase, with a tendency to saturation, was observed. Although the over-killing region deserves further investigation, the possibility of fitting the CL yields is an important feature for hadrontherapy, because it allows performing predictions also at LET values where experimental data are not available.

Finally, an approach was proposed to predict the ion-response of the cell line(s) of interest from the ion-response of a reference cell line and the photon response of both. A pilot study on proton-irradiated AG01522 and U87 cells, taking V79 cells as a reference, showed encouraging results.

Keywords: hadrontherapy, biophysical models, Monte Carlo simulations, Relative Biological Effectiveness, cell survival

1.Introduction

Hadrontherapy is spreading more and more rapidly worldwide, with more than 150,000 patients treated till now, more than 70 facilities in operation, and more than 60 centres under construction or in a planning stage (http://www.ptcog.ch). The rationale underlying the use of protons and Carbon ions, and possibly other charged particles including He- and O-ions (Tommasino et al 2015), mainly relies on their physical properties, which allow localizing most of the dose in the tumor region thanks to the so-called Spread-Out Bragg Peak (Amaldi and Kraft 2005). Furthermore, the biological effectiveness of heavier ions like Carbon is significantly higher than that of photons, which makes these ions particularly suitable for the treatment of radio-resistant tumours.

Since for heavier ions the biological effectiveness increases with depth in tissue, a description of such increase needs to be integrated in the various Treatment Planning Systems, as well as the radiation transport codes used for research and/or plan recalculation, like FLUKA (Battistoni et al 2016), PHITS (Sato et al 2014) and GEANT4 (Allison et al 2016). In principle, such description can be based either on experimental studies, or on biophysical models. While at NIRS in Chiba (Japan) a semi-empirical approach was adopted, at HIT in Heidelberg (Germany) and CNAO in Pavia (Italy) the Local Effect Model, or LEM (e.g. Scholz and Kraft 1994), is applied for Carbon therapy. This kind of models can be useful also for protons: although a constant Relative Biological Effectiveness (RBE) of 1.1 is assumed in clinics, according to several studies this approach may be sub-optimal. Many *in vitro* and *in vivo* experimental works show that proton RBE increases significantly in the SOBP distal region, due to an excess of protons having low energy and thus higher LET (e.g. Paganetti et al 2002, Paganetti and van Luijk 2013, Chaudhary et al 2014, Michaelidesová et al 2017). An extensive analysis of proton RBE experiments can be found in (Grun et al 2017), where the predictions of the Local Effect Model are compared with many *in vitro* and *in vivo* data taken from the literature.

In addition to LEM, many biophysical models have been proposed, including the Microdosimetric-Kinetic Model (MKM) used in Japan (e.g. Kase et al 2006) and more recent approaches specific for protons, like those developed by Tilly et al (2005), Carabe et al (2012), Wedenberg et al (2013) and McNamara et al (2015). A discussion on these models, which is beyond the scope of this paper, can be found in Carante and Ballarini (2017).

In this work, an upgraded version of the BIANCA II biophysical model developed in Pavia (Carante and Ballarini 2016) was applied to V79 and AG01522 cells exposed to protons, C-ions and He-ions over a wide LET interval (0.6-30.5 keV/μm for protons, 22.5-502 keV/μm for C-ions, and 16.2-132 keV/μm for He-ions), as well as proton-irradiated U87 cells. In the following, after summarizing the main characteristics of the model, the results obtained for cell survival will be presented, and the possibility of performing full predictions in the framework of hadrontherapy will be discussed.

2.Methods

This work was performed by means of a biophysical model, implemented in the form of a Monte Carlo simulation code, that initially was specific for radiation-induced chromosomal aberrations (e.g. Ottolenghi et al 1999, Ottolenghi et al 2001, Ballarini and Ottolenghi 2004, Ballarini and Ottolenghi 2005), and later has been extended to cell death (Ballarini 2010, Ballarini et al 2013, Ballarini et al 2014, Carante et al 2015, Carante and Ballarini 2016, Ballarini and Carante 2016). This extended

version, which has been named BIANCA (BIophysical ANalysis of Cell death and chromosome Aberrations), provides simulated cell survival curves, as well as chromosome aberration dose-response curves, following *in vitro* exposure to different radiation types. The model makes use of two adjustable parameters that have a specific biophysical meaning (see below). Although several mechanisms are not described explicitly to avoid the introduction of further parameters, some key steps of the process leading from energy deposition by radiation to chromosome damage and cell death are taken into account.

2.1 Model assumptions

The basic idea underlying the BIANCA approach is that some DNA damage types (called "Cluster Lesions", or CLs) lead to chromosome aberrations *via* distance-dependent mis-rejoining, or un-rejoining, of chromosome fragments, and that some chromosome aberrations (dicentrics, rings and large deletions, as discussed below) lead to clonogenic cell death. A CL is defined as a damage of the double-helix that is severe enough to produce two independent chromosome fragments. A cluster of DSBs may be a good candidate as this severe damage (e.g. Campa et al 2009, Schipler and Iliakis 2013, Carante et al 2015). However, since the characterization of such critical lesions is still an open question in the radiobiology community, we purposely decided not to give an *a priori* definition of "cluster lesions", and the CL yield (mean number of CLs per Gy and per Dalton, which can be easily converted into CLs per Gy and per cell) is an adjustable parameter. The value of this parameter, which influences the absolute value of the surviving fraction at the various doses rather than the shape of the survival curve, mainly depends on particle type and energy. However, the CL yield is also modulated by the target cell features: in general, more radioresistant cells (i.e. with higher surviving fractions, like V79 cells) require lower CL yields than radiosensitive or normal cells (i.e. with lower surviving fractions, like AG01522 cells).

Although it is widely accepted that chromosome-fragment (mis-)rejoining is a distance-dependent process, the features of such distance-dependence still represent an open question. For the sake of simplicity, a step function has been adopted in this work and in all previous works on cell survival, although a negative exponential function has been introduced in a recent work on chromosome aberrations (Tello et al. 2017, Tello et al. 2018). More specifically, two chromosome free-ends with initial distance smaller than a cut-off value d will undergo end-joining with 100% probability, whereas two fragments with initial distance larger than d will never undergo end-joining. Although this approximation does not reflect the existing bias for intra-arm relative to inter-arm chromosome exchanges, it allows reproducing the yield of lethal aberrations (dicentrics plus rings plus deletions), which is what counts for simulating cell death. In the first model version (e.g. Ballarini et al. 2013, Ballarini et al. 2014, Carante et al. 2015), which from now on will be called BIANCA I, the cut-off distance was an adjustable parameter. On the contrary in the subsequent version, called BIANCA II (Carante and Ballarini 2016, Ballarini and Carante 2016, Carante and Ballarini 2017, Testa et al. 2018), d has been fixed to the mean distance between two adjacent chromosome territories, which resulted to be ~3.6 μm for V79 cells and be ~3.0 μm for AG01522 cells. The expression "chromosome territory" refers to a region of the cell nucleus where a given chromosome is localized during interphase (Cremer et al 1996). This choice was based on nuclear architecture studies, which suggest that DNA repair mainly occurs at the boundaries of chromosomal and sub-chromosomal domains (Cremer et al 1996). In BIANCA II a fragment un-rejoining probability, called f, has been introduced to take into account that not all fragments are eventually rejoined with a partner (Wu et al 1999, Wu et al 2002), even in the presence of potential "partners" within the cut-off distance d. According to these studies the un-rejoining probability should be cell-line-dependent, because radio-sensitive cells tend to show higher frequencies of un-rejoined fragments than normal or radio-resistant cells (Cornforth and Bedford 1985). Although some works report an increase of incomplete chromosome exchanges with LET (Wu et al 2002), others do not show any LET-dependence (Wu et al 1999).

Therefore the value of *f*, which is the second and last adjustable parameter in BIANCA II, is assumed to be cell-line-dependent but independent of radiation quality. Different from the CL yield, the un-rejoining probability influences the shape of the survival curve: in general, a cell line with a lower α/β ratio requires a lower *f* value, whereas a line with a higher α/β ratio requires a higher *f* value.
The assumption linking chromosome aberrations to cell death reflects the observed relationship between the so-called "asymmetrical aberrations" (dicentrics, rings and deletions) and clonogenic death that is reported in several studies (e.g. Carrano 1973, Cornforth and Bedford 1987). Since cell death can also derive from other pathways than chromosome aberrations, including apoptosis and necrosis, the current version of the model is specific for cell types in which such pathways do not play a relevant role, as is the case of V79 and AG01522 normal cells and of many tumour cells. More details on this issue can be found in (Carante and Ballarini 2017).

As reported elsewhere (Ballarini et al. 2013, Ballarini et al. 2014, Carante et al. 2015), BIANCA I has been applied to V79 cells exposed to photons, protons (LET: 10.1-27.6 keV/μm), C-ions (LET: 13-339 keV/μm) and He-ions (LET: 20-120 keV/μm), as well as AG01522 cells exposed to photons, protons (LET: 1.1-22.6 keV/μm), C-ions (LET: 48.8 and 147.6 keV/μm) and Fe-ions (LET: 300 keV/μm). For both cell types, d=5 μm allowed to obtain a general correspondence between simulated and experimental survival curves. However, the effectiveness of high-LET radiation at low doses was underestimated, and, more importantly, at the higher LET values the simulated survival curves showed a slope decrease at higher doses. This may be related to the high value used for d, which was not very realistic because it was higher than most estimates available in the literature. Following the development of BIANCA II, new comparisons with chromosome aberration data have been performed. Good agreement was found not only for total aberrations, but also for different aberration types (dicentrics, rings and excess acentric fragments) considered separately. Concerning cell survival, up to now BIANCA II has been applied to V79 and AG01522 cells exposed to photons and protons (LET: 7.7-27.6 keV/μm for V79 cells, 1.1-22.6 keV/μm for AG01522 cells) (Carante and Ballarini 2016, Ballarini and Carante 2016). The agreement between simulations and data was satisfactory, except for a tendency to underestimate the surviving fraction at the higher doses.

In the present work, an upgraded version of BIANCA II was applied, where "upgraded" means that: i) interphase chromosome-arm domains, which previously were described only implicitly, were modelled explicitly, leading to more than 97% of fidelity with respect to each chromosome-arm DNA content (Tello et al. 2017, Tello et al. 2018); ii) cell death was calculated on a cell-by-cell basis (see below), whereas previously a Poisson distribution of lethal aberrations was assumed. Like in previous works, V79 nuclei were modelled as cylinders of circular base (with 6-μm height and 6-μm radius), whereas AG01522 nuclei were represented as cylinders of elliptical base (with 4-μm height, 20-μm major axis and 10-μm minor axis). The mean distance between two adjacent chromosome territories resulted to be 3.8 μm for V79 cells, and 3.0 μm for AG01522 cells.

2.2 Main simulation steps

The starting information for simulating cell survival and chromosome aberration induction at dose D is the Cluster Lesion yield, i.e. the mean number of CLs per Gy and per cell. For each cell exposed to a given dose of sparsely-ionizing radiation, like X- or γ-rays, an actual number of CLs is then extracted from a Poisson distribution, and these CLs are uniformly distributed in the nucleus volume.

On the contrary for ion irradiation, which is assumed to be parallel to the axis of the cylinder that represents the nucleus, the mean number of primary particles traversing a nucleus at dose D is calculated as

$$N = D \cdot S/(0.16\ L) \quad (1)$$

where D is the absorbed dose in Gy, *S* is the nucleus cross-sectional area in μm^2, *L* is the radiation LET in keV/μm, and 0.16 is a factor due to the conversion of eV into Joules, assuming a nucleus density of 1 g/cm^3. For each cell, an actual number of traversals is then extracted from a Poisson distribution, and the mean number of CLs per traversal is calculated as

$$CL/track = 0.16 \cdot CL \cdot Gy^{-1} \cdot cell^{-1} \cdot L \cdot S^{-1} \quad (2)$$

To make comparisons between cell types that have a different nucleus thickness, it is also useful to express the CL yield as the mean number of CLs per unit traversal length. In the case of a cylindrical nucleus, this quantity is expressed by

$$CL/\mu m = 0.16 \cdot CL \cdot Gy^{-1} \cdot cell^{-1} \cdot L \cdot V^{-1} \quad (3)$$

where V is the nucleus volume in μm^3.

For each nucleus traversal, an actual number of CLs is then extracted from a Poisson distribution. For (low-energy) protons and He-ions these CLs are uniformly distributed along the segment that represents the trajectory of the primary particle. On the contrary for heavier ions some CLs are "shifted" radially to model the effects of the so-called "delta rays", i.e. high-energy secondary electrons. More specifically, each CL is assumed to have a 0.5 probability to be induced along the primary-ion trajectory, and a 0.5 probability to be shifted radially. This 0.5 value is an application of the idea that half of the total energy deposition derives by excitations and electron plasma oscillations, which mainly occur in the track core, whereas the remaining half derives from ionizations induced by secondary electrons, which mainly occur in so-called "penumbra" region (Chatterjee and Schaefer 1976). The fact that this approximation may lead to some incongruities at the core/penumbra interface does not affect the simulation outcomes, because the relevant information is whether a given CL falls in a certain chromosome territory or in another one, which is a micrometre-scale question. For those CLs that are shifted, the probability to be induced at distance *r* from the primary particle is taken as proportional to 1/r. The maximum radial distance is set equal to the maximum range of secondary electrons, which is calculated according to

$$r_{max}\ (\mu m) = \gamma \cdot E^{1.7} \quad (4)$$

where E is the projectile energy in MeV/u and $\gamma = 0.062\ \mu m\ (MeV/u)^{-1.7}$ (Kiefer and Straaten 1986).

After distributing the various CLs in the nucleus volume, the subsequent simulation steps consist of: identification of the chromosome and the chromosome-arm that was hit by each CL; un-rejoining or distance-dependent (mis-)rejoining of chromosome fragments; scoring of different aberration types. During aberration scoring, chromosome fragments that have a DNA content smaller than 3 Mega-base-pairs (Mbp) are not considered, because they are not visible in metaphase under Giemsa staining (Cornforth and Bedford 1987). A discussion on the role of this value can be found in (Carante et al 2015). The whole procedure is then repeated for many runs, until the required statistical precision is reached. In this work, where we required that the relative error on the surviving fraction was not larger than 5%, the simulations corresponding to the lower surviving fractions were performed with 200,000 runs.

At the end of the last run the surviving fraction is calculated, as well as the mean number of chromosome aberrations per cell. In previous works, the surviving fraction has been calculated as

$$S(D) = \exp[-LA(D)] \qquad (5)$$

where LA(D) is the mean number of "Lethal Aberrations" (dicentrics plus rings plus large deletions) per cell at dose D. This implies that the number of lethal aberrations follows a Poisson distribution, which at low- and intermediate-LET is a reasonable approximation, but at high LET it does not hold any more. As mentioned above, in the present work the surviving fraction was thus calculated on a cell-by-cell basis: a cell with (at least) one lethal aberration was counted as a dead cell, whereas a cell with zero lethal aberrations was counted as a surviving cell. While for photons and protons the two approaches were basically equivalent, for heavier ions a significant difference was found, and calculating S on a cell-by-cell basis led to a better agreement with the experimental data (see below).

3.Results and Discussion

As mentioned in the introduction, in this work the upgraded BIANCA II was applied to V79 cells, which have a low α/β ratio and are widely used both in basic radiobiology and in the characterization of hadrontherapy beams, and to AG01522 cells, which are normal human fibroblasts characterized by a high α/β ratio. Sections 3.1, 3.2 and 3.3 report the results obtained for protons, C-ions and He-ions, respectively. In section 3.4 we propose an approach for performing full predictions (without any parameter adjustment) for the cell line(s) of interest starting from a cell line chosen as a reference.

3.1 Protons

A comparison of BIANCA II simulations with survival data on V79 cells exposed to different proton beams, taken from Folkard et al (1996) and Belli et al (1998), has been published in a previous paper (Carante and Ballarini 2016). In the present work, those simulations were repeated applying the BIANCA II upgraded version, where chromosome-arm domains are modelled explicitly and cell survival is calculated on a cell-by-cell basis.

Figure 1 reports simulated survival curves for four LET values (7.7, 11.0, 20.0 and 30.5 keV/μm), as well as X-rays as a reference radiation. The experimental data for comparison were taken from Belli et al (1998). Simulations at 10.1, 17.8 and 27.6 keV/μm were also performed, and the outcomes showed good agreement with the data reported in Folkard et al (1996). More specifically, at 10.1 and 17.8 keV/μm the value of the reduced chi-square was 0.6 and 1.9, respectively. At 27.6 keV/μm the agreement for the entire curve, which extends to doses that are much higher than those used in hadrontherapy fractions, was worse (with a reduced chi-square of 11.8); however, limiting the comparison at doses not higher than 4 Gy the reduced chi-square was 1.7. These results were not included in figure 1 to avoid making the figure too "crowded".

All the curves for V79 cells were obtained with f =0.08, based on a previous work (Carante and Ballarini 2016). The yield of Cluster Lesions was adjusted separately for each LET value. For the X-ray curve a yield of 4.3 $CL \cdot Gy^{-1} \cdot cell^{-1}$ was used, whereas the proton curves were obtained with CL yields in the range ~0.004 – 0.025 CL/μm, increasing with LET. Except for the highest LET value, where the slope at high doses of the simulated curve is more pronounced with respect to the data, the agreement was satisfactory, since in most cases the simulations were within the experimental error, and the reduced chi-square was between 1.1 and 1.9.

The underestimation of the surviving fraction at the higher doses (especially at the higher LET values) is suggestive of an over-estimation of the so-called "inter-track effects". This might be related to the choice adopted for the fragment end-joining probability, which was modelled by a step function with threshold distance in the order of the linear dimensions of interphase chromosome territories (that is, ~3.8 μm for V79 cells). At the higher doses, where a cell nucleus is traversed by many primary

particles, such choice may lead to an over-estimation of the interaction between two CL free-ends induced by two different primary particles. Adopting an end-joining probability that decreases monotonically with increasing the (initial) fragment distance, as we did in a very recent chromosome aberration study (Tello et al. 2017, Tello et al. 2018), might help overcoming this problem in future cell survival studies.

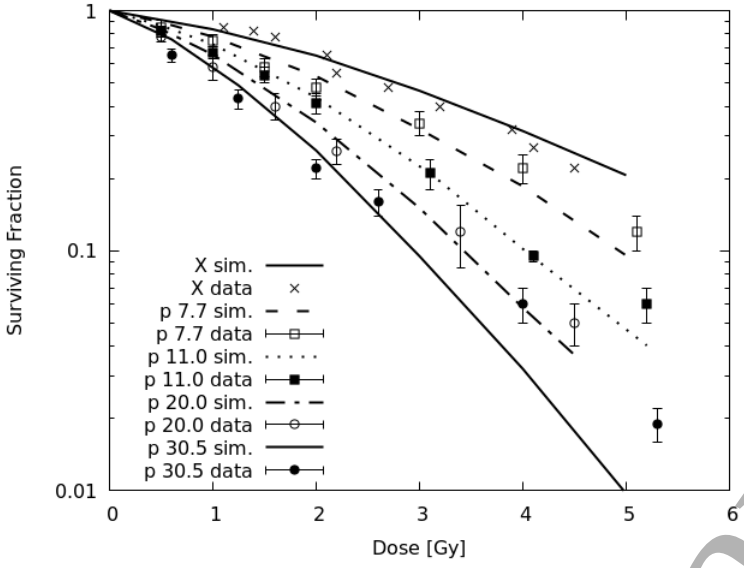

Figure 1. Survival of V79 cells irradiated with protons of different LET (7.7, 11.0, 20.0 and 30.5 keV/μm), as well as X-rays. The lines are simulation outcomes, the points are experimental data taken from Belli et al. (1998).

In Carante and Ballarini (2016) the model has been also applied to AG01522 normal human fibroblasts exposed to a proton beam available at the CATANA ocular melanoma facility of INFN-LNS in Catania, Italy (Cuttone et al 2011), where the cells were exposed at different depth positions corresponding to LET values in the range 1.1 - 22.6 keV/μm (Chaudhary et al 2014). Like for V79 cells, in the present work those simulations were repeated making use of the upgraded BIANCA II, and the results were in line with those reported in Carante and Ballarini (2016).

Furthermore, a subsequent work by the same group of authors was considered (Marshall et al. 2016), in which AG01522 cells were irradiated at four key depth positions of a clinical SOBP available at the Proton Therapy Center in Prague, Czech Republic. The corresponding LET values were 0.63, 1.68, 2.45 and 7.50 keV/μm. Figure 2 reports simulated survival curves for these four LET values. The corresponding experimental data, taken from Marshall et al. (2016), are also reported for comparison. Based on (Carante and Ballarini 2016), all simulations for AG01522 cells were performed with f = 0.18. Again, the yield of cluster lesions was adjusted separately for each LET value. The curves reported in figure 2 were obtained using CL yields in the range ~0.001 – 0.011 CL·μm^{-1}, increasing with LET. With these values, the agreement between simulation outcomes and experimental data was quite satisfactory, since all simulations were within the error bars reported in the experimental work, and the value of the reduced chi-square was smaller than 1 for all curves.

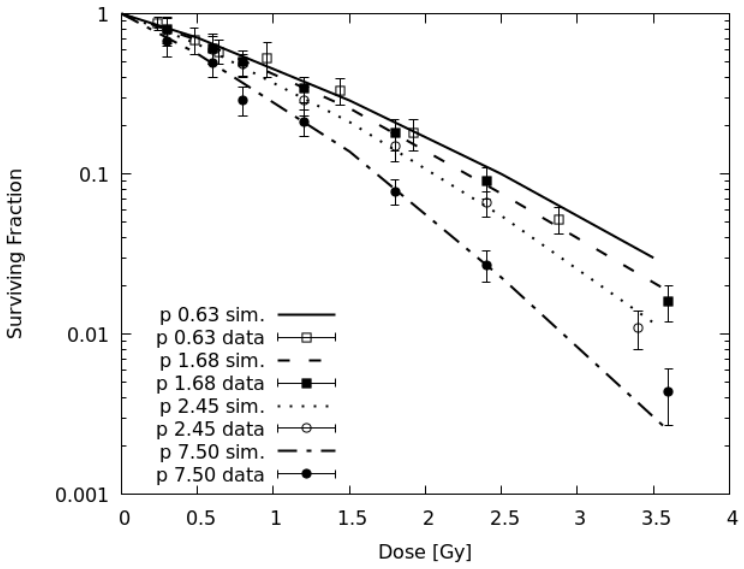

Figure 2. Survival of AG01522 cells irradiated with protons of different LET (from top to bottom: 0.63, 1.68, 2.45 and 7.50 keV/μm). The lines are simulation outcomes, the points are experimental data taken from Marshall et al. (2016)

The CL yields (mean number of CLs per unit length along the primary-particle traversal) used to simulate the survival of proton-irradiated V79 and AG01522 cells are reported in figure 3 as a function of LET. For both cell lines the CL yield increased with LET, consistent with the increasing clustering of energy deposition in the target. For a given LET value, a higher CL yield was used for AG01522 cells with respect to V79 cells, reflecting the higher radiosensitivity of AG01522 cells.
For both cell lines the LET-dependence of the CL yield was well described by a linear-quadratic function of the form $Y(L) = aL + bL^2$, where Y is the CL yield expressed in CL/μm, L is the radiation LET in keV/μm, and a and b are fitting parameters. To evaluate the fit goodness, we assigned to each CL yield a 5% relative error, equal to the maximum relative error of the simulated surviving fraction. Such CL fitting allows deriving CL yields, and thus predicting survival curves, even at LET values where experimental data are not available. This is important in view of applications in hadrontherapy, where the biological effectiveness along the beam profile should be known at as many depth positions as possible, that is as many LET values as possible.
Interestingly, the two fitting curves showed a very similar shape: *a posteriori,* we realized that by multiplying the CL fitting function of V79 cells by a fixed factor, one obtains a function that fits reasonably well the CL yields of AG01522 cells. The possible implications will be discussed in section 3.4.

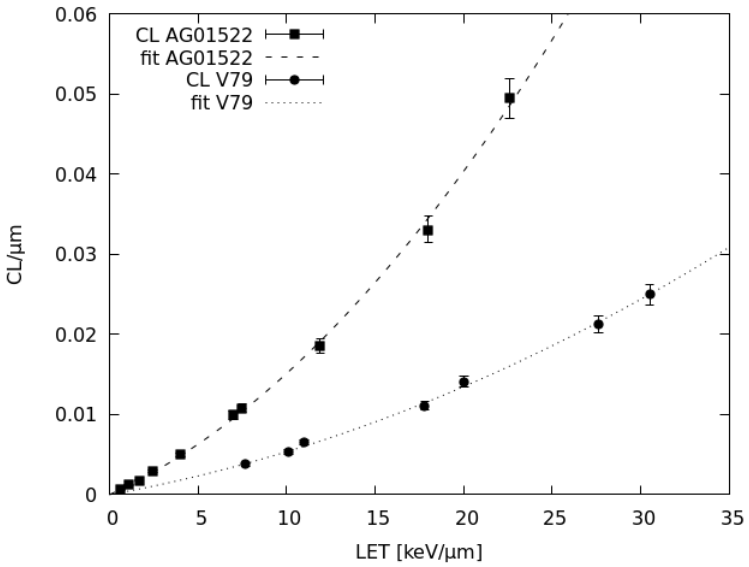

Figure 3. Cluster Lesion yields used to simulate the survival of proton-irradiated V79 cells (lower line and points) and AG01522 cells (upper line and points). Each point represents the mean number of CLs per micrometer used as a code input, whereas the lines are linear-quadratic fits. A 5% relative error was assigned to each CL yield.

3.2 Carbon ions

The approach was then extended to Carbon ions. For V79 cells the data reported in Furusawa et al. (2000) were considered, which cover a very wide LET range (22.5 – 502 keV/µm). Keeping $f = 0.08$ and adjusting the CL yield for each LET value, simulated survival curves were obtained for all 24 LET values reported in the experimental paper. To avoid making the figures too difficult to read, only some of them were reported in figures 4a and 4b. Figure 4a also shows the X-ray curve as a reference.

CL yields in the range ~0.009 – 0.556 CL/µm provided simulation outcomes in good agreement with the experimental results obtained by Furusawa et al. (2000), who fitted each survival curve by a linear-quadratic function of the form $S(D) = \exp(-\alpha D - \beta D^2)$. The paper reports the α coefficient and the D_{10} coefficient (dose at 10% survival), from which we derived the β coefficient. Concerning the 16 curves that are not shown in figures 4a and 4b, for 11 of them the maximum percentage displacement between simulated curve and data fit was ~30%, for four of them it was ~50-60%, and only for the remaining one the agreement was worse. The LET-dependence of the CL yield will be discussed below.

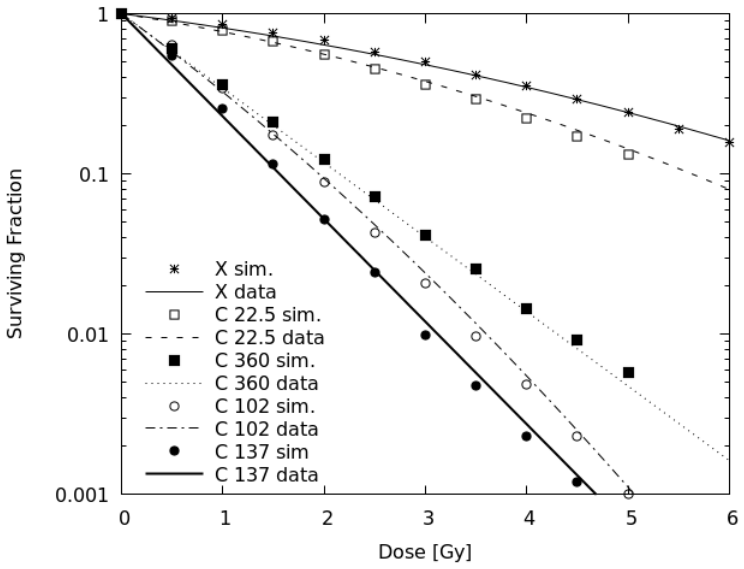

Figure 4(a). Survival of V79 cells irradiated by Carbon beams of different (dose-averaged) LET (22.5, 360.0, 102.0 and 137.0 keV/μm), as well as X-rays as a reference. The points are simulation outcomes, whereas the lines are experimental data fits of the form $S(D) = \exp(-\alpha D - \beta D^2)$ taken from Furusawa et al. (2000).

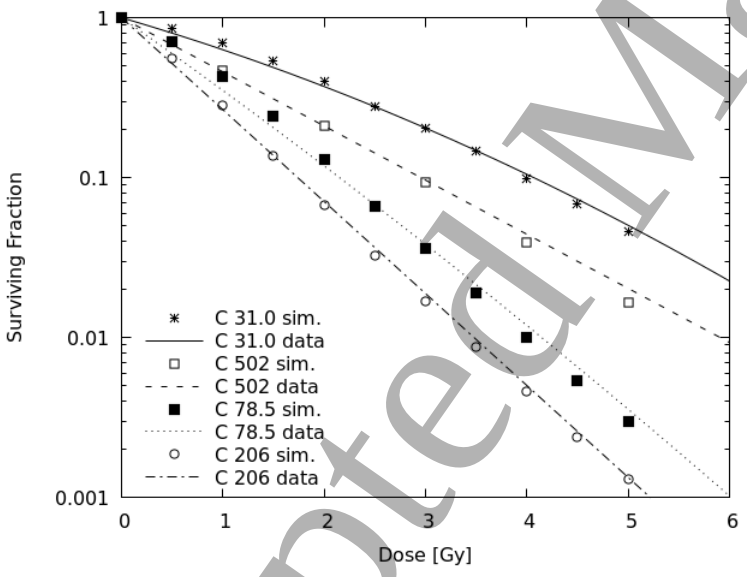

Figure 4(b). Survival of V79 cells irradiated with Carbon beams of different (dose-averaged) LET (from top to bottom: 31.0, 502.0, 78.5 and 206.0 keV/μm). The points are simulation outcomes, whereas the lines are experimental data fits of the form $S(D) = \exp(-\alpha D - \beta D^2)$ taken from Furusawa et al. (2000)

For Carbon-irradiated normal human fibroblasts we considered the data reported by Hamada et al. (2006), who irradiated AG01522 cells with Carbon beams of 76.3 keV/μm and 108.0 keV/μm, and Kavanagh et al. (2013), who irradiated AG01522 cells with Carbon beams of 48.8 keV/μm and 147.6 keV/μm.

Figure 5 reports simulated survival curves for Carbon beams with these four LET values. Like for proton-irradiated AG01522 cells, all the curves reported in figure 5 were obtained with $f = 0.18$ based on a previous work (Carante and Ballarini 2016). Following adjustment of the CL yield for each LET value, CL yields in the range 0.052 – 0.354 CL/μm provided simulation outcomes in good agreement with the considered data, since the simulations were within the experimental error bars with the only exception of the point at the highest dose for 147.6 keV/μm. However, this point is also much lower than the fitting function reported in the experimental paper. At 48.8, 108.0 and 147.6 keV/μm (excluding the point at the highest dose for 147.6 keV/μm) the reduced chi-square was between 1.1 and 1.7. At 76.3 keV/μm the reduced chi-square was much higher (8.2), but it should be taken into account that only three experimental points were available, and the first one had a very small error bar.

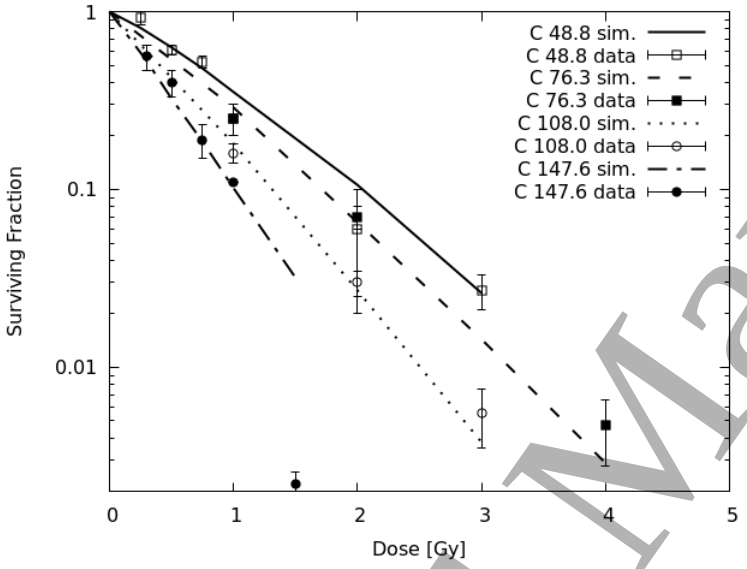

Figure 5. Survival of AG01522 cells irradiated by Carbon beams of different LET (from top to bottom: 48.8, 76.3, 108.0 and 147.6 keV/μm). The lines are simulation outcomes, whereas the points are experimental data taken from Hamada et al. 2006 (76.3 keV/μm and 108.0 keV/μm) and Kavanagh et al. 2013 (48.8 keV/μm and 147.6 keV/μm).

The LET-dependence of the CL yield (mean number of Cluster Lesions per μm) for Carbon ions is illustrated in figures 6a and 6b. Figure 6a shows the CL yield used for V79 and AG01522 cells irradiated by C-ions with LET below 150 keV/μm, thus excluding the over-killing region shown by V79 cells at higher LET. In this LET interval, like for protons the LET-dependence of the CL yield was well described by a linear-quadratic function of the form $Y(L) = aL + bL^2$ for both cell lines. Moreover, the function obtained by multiplying the V79 fitting function by a fixed factor, fits reasonably well the CL yields of AG01522 cells. For each of the two cell lines, the CL fitting function used for Carbon was lower than that used for protons. This is consistent with the fact that heavier ions, which at a given LET have higher-energy secondary electrons, have a wider track, and thus are less effective in inducing DNA cluster damage.

Figure 6b analyzes the whole LET interval considered for V79 cells, which showed the so-called overkilling phenomenon above ~150 keV/μm. Interestingly, while above ~150 keV/μm the mean

number of CLs per unit dose ($CL \cdot Gy^{-1} \cdot cell^{-1}$) starts decreasing, the mean number of CLs per unit track length ($CL \cdot \mu m^{-1}$) continues to increase (although less rapidly), until it seems to reach a plateau. This can be explained by considering the relationship reported in eq. (3), according to which the mean number of CLs per unit track length is proportional to the product between the mean number of CLs per unit dose and the radiation LET. Due to the less rapid increase of the yield of CLs per micrometer in the over-killing region, the linear-quadratic fit was not applicable to the entire LET interval (22.5 – 502 keV/μm). Although this issue deserves further investigation in the future, it is worth mentioning that, for instance, a function of the form $c \cdot \text{arctg}\,(a \cdot L + b \cdot L^2)$ provided a much better fit, as shown in figure 6b.

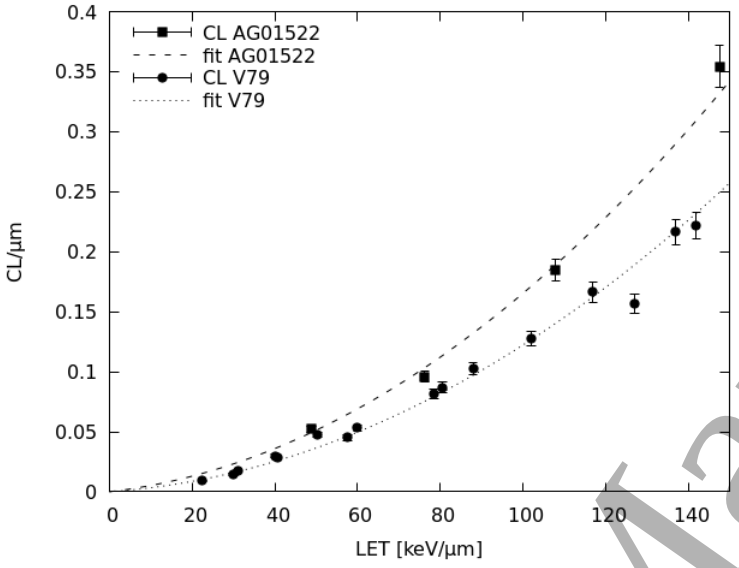

Figure 6(a). Cluster Lesions yields used to simulate the survival of Carbon-irradiated AG01522 cells (upper line and points) and V79 cells (lower line and points) up to ~150 keV/μm. Each point represents the mean number of CLs per micrometer used as a code input, whereas the lines are linear-quadratic fitting functions. A 5% relative error was assigned to each point.

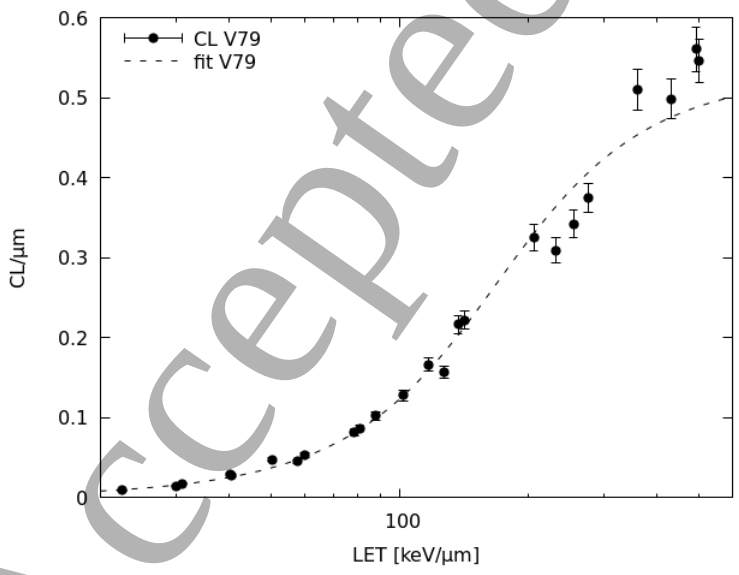

Figure 6(b). Cluster Lesions yields used to simulate the survival of Carbon-irradiated V79 cells over the whole LET range (22.5 - 502 keV/μm). Each point represents the mean number of CLs per micrometre used as a code input, whereas the line is a fit of the form $c \cdot \mathrm{artg}(a \cdot L + b \cdot L^2)$. A 5% relative error was assigned to each point.

3.3 Helium ions

The model was then applied to Helium ions, for which there is a renewed interest in the hadrontherapy community (e.g., Mairani et al 2016). For V79 cells, we considered the paper by Furusawa et al. (2000) used for Carbon ions, which also reports data on V79 cells exposed to ^{3}He-ions over a LET range from 18.6 to 90.8 keV/μm. Survival curves were simulated for all 14 LET values reported in the experimental paper. To avoid making the figure too difficult to read, only some of them are reported in Figure 7. Like for protons and Carbon ions, all the curves for He-irradiated V79 cells were obtained with f =0.08. CL yields in the range ~0.009 – 0.132 CL/μm provided simulation outcomes in good agreement with the experimental data fits reported in Furusawa et al. (2000). Concerning the nine curves that are not shown in figure 7, for six of them the maximum percentage displacement between simulated curve and data fit was ~30%, for two of them it was ~50%, and only for the remaining one the agreement was worse.

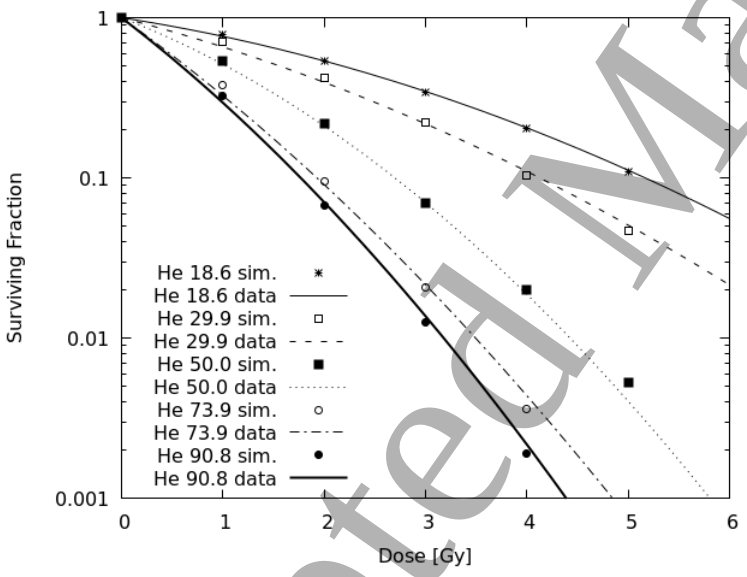

Figure 7. Survival of V79 cells irradiated by He-ion beams with different (dose-averaged) LET (from top to bottom: 18.6, 29.9, 50.0, 73.9 and 90.8 keV/μm). The points are simulation outcomes, whereas the lines are experimental data fits of the form $S(D) = \exp(-\alpha D - \beta D^2)$ taken from Furusawa et al. (2000).

Less data are available in the literature for He-ion-irradiated normal human fibroblasts. In this work we considered those reported by Hamada et al. (2006), who exposed AG01522 cells to ^{4}He ions of 16.2 keV/μm, and Neti et al. (2004), who irradiated AG01522 cells with ^{4}He ions of 132 keV/μm. Figure 8 reports simulated survival curves at these two LET values, together with the experimental data for comparison. Like for proton- and Carbon-irradiated AG01522 cells, the curves reported in figure 8 were obtained with f = 0.18. CL yields of 0.010 CL/μm (at 16.2 keV/μm) and 0.465 CL/μm

(at 132 keV/μm) provided a good correspondence with the considered data, since the simulations were within the error bars or very close to them, except for the two highest doses of the two curves. The reduced chi-square was 1.5 at 16.2 keV/μm, and 3.9 at 132 keV/μm.

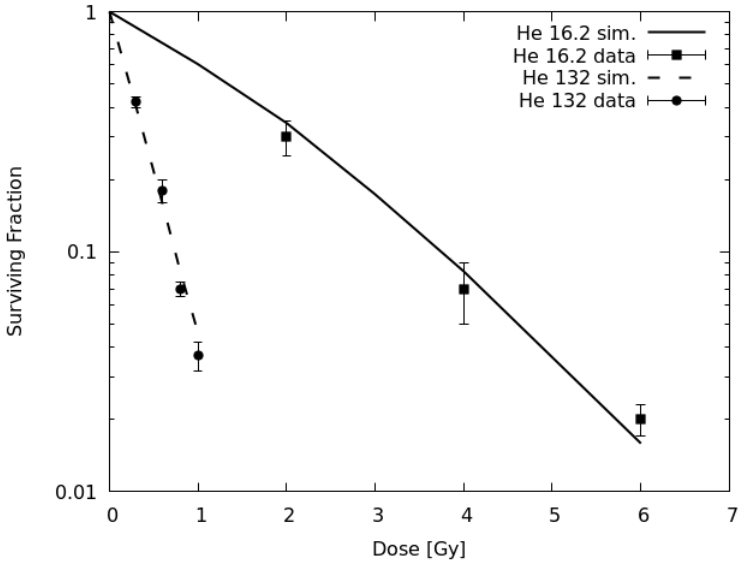

Figure 8. Survival of AG01522 cells irradiated by He-ion beams of 16.2 keV/μm (upper line and points) and 132 keV/μm (lower line and points). The lines are simulation outcomes, whereas the points are experimental data taken from Hamada et al. 2006 (16.2 keV/μm) and Neti et al. 2004 (132 keV/μm).

Figure 9 reports the mean number of Cluster Lesions per μm used to simulate the survival of He-irradiated V79 and AG01522 cells. For both cell lines the CL yield increased with LET in the considered LET interval, and it was well fitted by a linear-quadratic function of the form $Y(L) = aL + bL^2$. Also in this case, by multiplying the fit for V79 cells by a fixed factor, one obtains a function that fits well the CL yields of AG01522 cells. For each of the two cell lines, the CL fitting function used for He-ions was intermediate between the function used for protons and that used for C-ions. As discussed in section 3.2, this is consistent with the fact that different particles having the same LET have different track-structure properties, which make heavier particles less effective in the induction of DNA cluster damage.

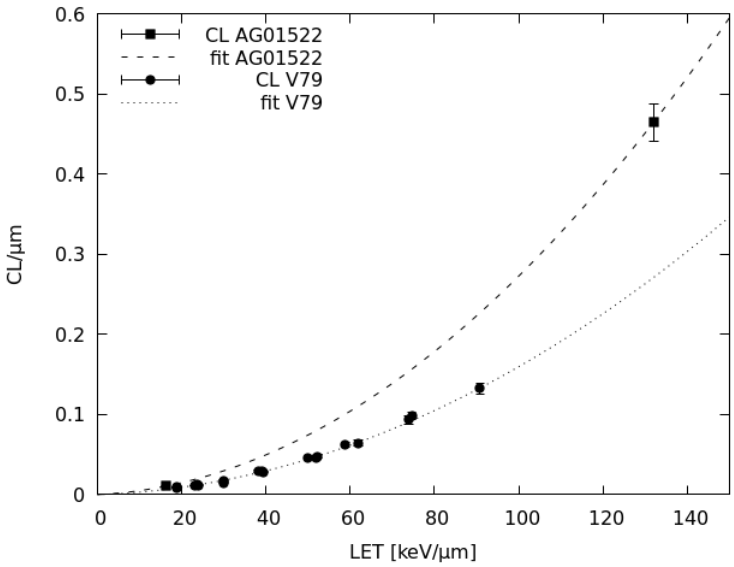

Figure 9. Cluster Lesion yields used to simulate the survival of He-ion-irradiated V79 cells (lower line and points) and AG01522 cells (upper line and points). Each point represents the mean number of CLs per micrometre used as a code input, whereas the lines are linear-quadratic fits. A 5% relative error was assigned to each CL yield.

3.4 Full predictions of ion-survival based on a reference cell line

As discussed above, in principle the CL yield for a given radiation quality (i.e., particle type and energy) should be adjusted separately for each considered cell line, since this parameter also depends on the target cell features: in general, for a given radiation quality, more radiosensitive cells require higher CL yields than less radiosensitive ones. However, as mentioned in the previous sections, the LET-dependence of the CL yield (mean number of CLs per unit traversal length) for the two considered cell lines showed a similar shape, since by multiplying the fitting function of V79 cells by a given factor we obtained reasonable fits for the CL yields of AG01522 cells. If this factor can be obtained by comparing the photon responses of the two cell lines, this would represent a further improvement of the model, since it would allow to fully predict the ion-survival of the cell line of interest based on the ion-survival of a reference cell line, as well as the photon-response of both.

To explore this possibility, we performed full predictions of proton survival for AG01522 cells based on the proton survival of V79 cells. More specifically, the mean number of CLs per µm to predict the survival of AG01522 cells at a given LET was derived by multiplying the value of the CL fitting function of V79 cells at that LET by the following factor:

$$[(CL\cdot Gy^{-1}\cdot cell^{-1})_{AG,X} / (CL\cdot Gy^{-1}\cdot cell^{-1})_{V79,X}] \cdot V_{V79}/V_{AG} \quad (6)$$

In the expression above, $(CL\cdot Gy^{-1}\cdot cell^{-1})_{AG,X}$ and $(CL\cdot Gy^{-1}\cdot cell^{-1})_{V79,X}$ are the photon CL yields used for AG01522 and V79 cells, respectively, whereas V_{AG} and V_{V79} are their nucleus volumes. According to eq. (3), the latter enter in the relationship linking the mean number of CLs per micrometre to the mean number of CLs per Gy and per cell. This formula therefore assumes that the ratio between the CL yields of the two cell lines is independent of LET.

For each of the proton LET values considered for AG01522 cells in figure 2 (0.63, 1.68, 2.45 and 7.50 keV/µm), we took the proton CL yield of V79 cells from the fit reported in figure 3, and we inserted in eq. (6) the X-ray CL yields of the two cell lines, as well as their nucleus volumes. Using

the CL yields for AG01522 cells obtained in this way, we ran simulations at these four LET values, and we compared the simulation outcomes – which are full predictions performed without any parameter adjustment – with the experimental data reported in figure 2.

Figures 10a and 10b report the obtained results. In spite of a general tendency to overestimate the survival at 7.5 keV/μm, for the other three LET values the predictions were in very good agreement with the data: the simulation outcomes were within the experimental error bar for each considered experimental point with a single exception (the highest dose at 2.45 keV/μm), and the reduced chi-square was smaller than 0.7.

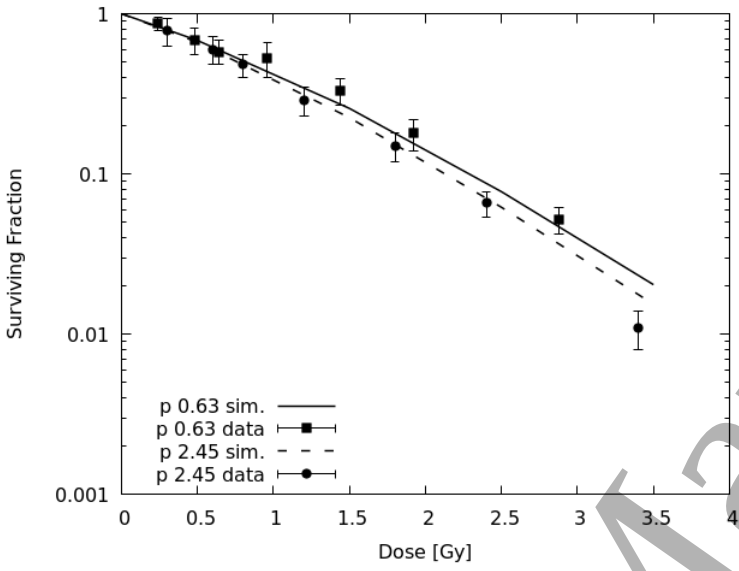

Figure 10(a). Survival of AG01522 cells irradiated by protons of 0.63 keV/μm (upper line and points) and 2.45 keV/μm (lower line and points). The lines are model full predictions (see the text for the details), the points are experimental data taken from Marshall et al. (2016)

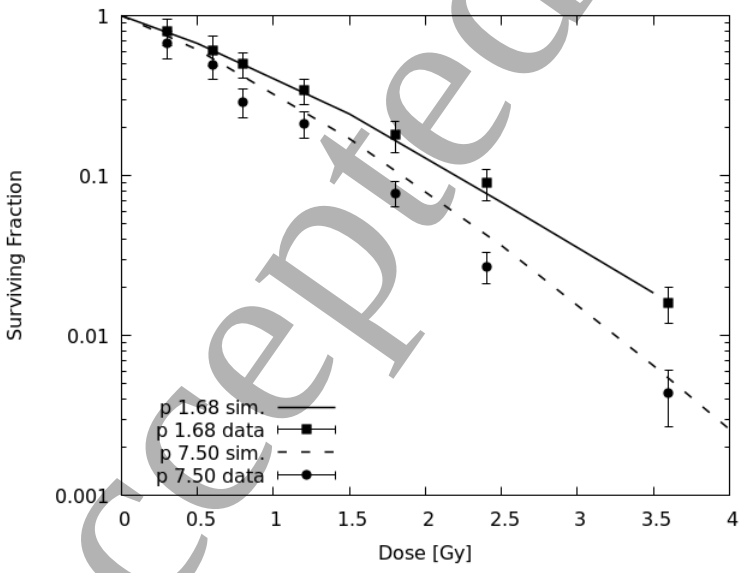

Figure 10(b). Survival of AG01522 cells irradiated by proton beams of 1.68 keV/μm (upper line and points) and 7.50 keV/μm (lower line and points). The lines are model full predictions (see the text for the details), the points are experimental data taken from Marshall et al. (2016)

To test if this method can be extended to other cell lines, the approach described above was also applied to proton-exposed U87 glioma cells. The experimental data for comparison were taken from the work by Chaudhary et al. (2014), who irradiated U87 cells (as well as AG01522 cells, as discussed above) at six depth positions (corresponding to LET values in the range 1.1 - 22.6 keV/μm) of a therapeutic proton beam available at INFN-LNS in Catania, Italy. The nucleus of U87 cells was modelled by a cylinder with circular base, with a 98.6 μm^2 nuclear area and a 7.7 μm thickness *(Berardinelli, personal communication).* Since in these cells the modal number of chromosomes is 44, very similar to the chromosome content of normal (human) cells, the number of chromosomes in the nucleus was left unchanged with respect to the AG01522 simulations. Analogous to AG01522 cells, the proton CL yields to perform full predictions of U87 cell survival were obtained by multiplying the V79 (proton) CL yield by the following factor, which is analogous to that reported in eq. (6):

$$[(CL\cdot Gy^{-1}\cdot cell^{-1})_{U87,X} /(CL\cdot Gy^{-1}\cdot cell^{-1})_{V79,X}] \cdot V_{V79}/V_{U87} \quad (7)$$

The photon CL yield for U87 cells, as well as their chromosome fragment un-rejoining probability *f*, was adjusted to the X-ray curve reported in Chaudhary et al. (2014). 2.3 $CL\cdot Gy^{-1}\cdot cell^{-1}$ and $f = 0.03$ provided a very good agreement with the experimental data, since the reduced chi-square was 0.9.

The full predictions for the six considered LET values are reported in figures 11a and 11b. At the four lower LET values (1.1, 4.0, 7.0 and 11.9 keV/μm), good agreement was obtained between simulations and data, with a reduced chi-square between 0.3 and 1.7. At the two higher LET values (18.0 and 22.6 keV/μm), the simulations showed a tendency to underestimate the surviving fraction at the higher doses (as well as to overestimate it at low doses). As discussed in section 3.1, this seems to be a general behavior of the model at these intermediate LET values, which may be corrected in the future by applying a chromosome fragment end-joining probability that decreases monotonically with increasing the fragment distance. Furthermore, it is important to take into account that all simulations reported in figures 11a and 11b were performed without any parameter adjustment.

Although the proposed method cannot be generalized at this stage, because it needs to be tested for other cell lines and other radiation qualities, these results are encouraging in view of a future development of a fully-predictive model.

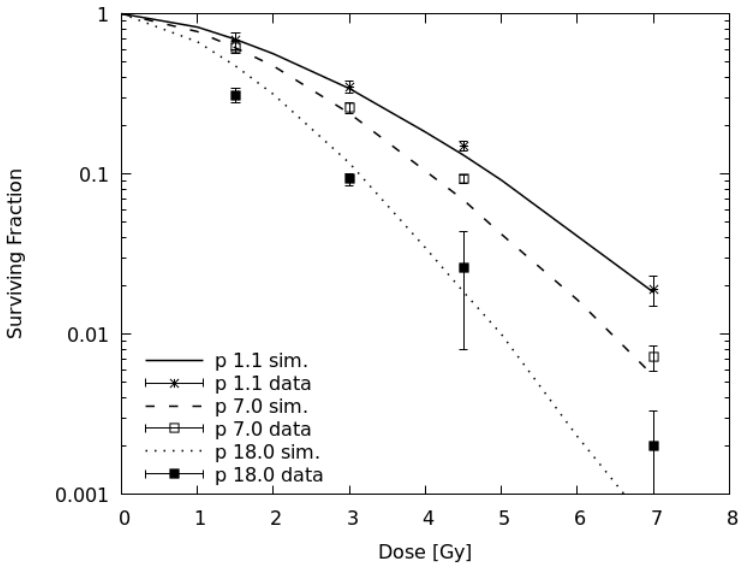

Figure 11(a). Survival of U87 cells irradiated by protons of different LET (from top to bottom: 1.1 keV/μm, 7.0 keV/μm and 18.0 keV/μm). The lines are full predictions (see the text for the details), the points are experimental data taken from Chaudhary et al. (2014)

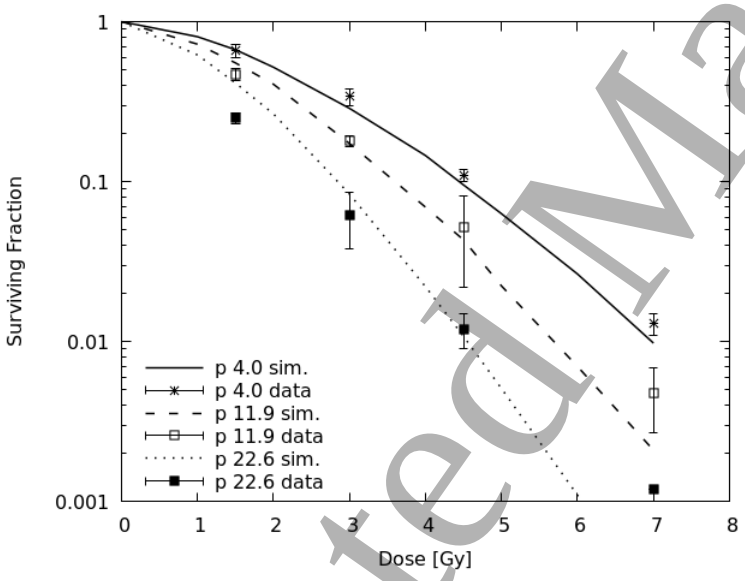

Figure 11(b). Survival of U87 cells irradiated by protons of different LET (from top to bottom: 4.0 keV/μm, 11.9 keV/μm and 22.6 keV/μm). The lines are full predictions (see the text for the details), the points are experimental data taken from Chaudhary et al. (2014)

Conclusions

An upgraded version of the BIANCA II model/code, with a more realistic description of interphase chromosome organization and of the link between chromosome aberrations and cell death, was applied to V79 and AG01522 cells exposed to protons, C-ions and He-ions over a wide LET interval, as well as proton-irradiated U87 cells.

The good agreement between simulations and experimental data suggests that the upgraded BIANCA II is suitable for calculating the biological effectiveness of hadrontherapy beams, especially considering that predictions can be performed also at LET values where there are no experimental data. In this framework, a work is in progress to develop an interface with the FLUKA radiation transport code.
Furthermore, an approach was proposed to fully predict the ion-survival of the cell line(s) of interest based on the ion-survival of a reference cell line, and the photon response of both. A pilot study on proton-irradiated AG01522 and U87 cells showed promising results.
Concerning the further improvement of the model, in the future we plan to extend it to other cell lines (especially other tumor cells) and possibly other radiation types (e.g., Oxygen ions). Furthermore, it is desirable to include in the model a description of other forms of cell death than mitotic death, such as apoptosis, which can be important for evaluating the response of normal tissues. The approach proposed to perform full predictions also deserves further investigation to verify if it can be generalized to other radiation qualities, as well as other cell lines.

Acknowledgements

This work was supported by the Italian National Institute of Nuclear Physics (projects “ETHICS” and “MC-INFN”). M P Carante’s activity was supported by the FLUKA collaboration. The authors are also grateful to A. Antoccia, F. Berardinelli and C. Dappiaggi for useful discussions.

References

Allison J *et al* 2016 Recent Developments in Geant4 *Nucl. Instr. Meth. A* **835** 186-225

Amaldi U and Kraft G 2005 Radiotherapy with beams of carbon ions *Rep. Prog. Phys.* **68** 1861–1882

Ballarini F 2010 From DNA Radiation Damage to Cell Death: Theoretical Approaches *J. Nucleic Acids* **2010** 350608

Ballarini F, Altieri S, Bortolussi S, Giroletti E and Protti N 2013 A Model of Radiation-Induced Cell Killing: Insights into Mechanisms and Applications for Hadron Therapy *Radiat. Res.* **180** 307–315

Ballarini F, Altieri S, Bortolussi S, Carante M, Giroletti E and Protti N 2014 The BIANCA model/code of radiation-induced cell death: application to human cells exposed to different radiation types *Radiat. Environ. Biophys.* **53** 525–533

Ballarini F and Carante MP 2016 Chromosome aberrations and cell death by ionizing radiation: evolution of a biophysical model *Radiat. Phys. Chem.* **128** 18-25

Ballarini F and Ottolenghi A 2004 A model of chromosome aberration induction and CML incidence at low doses *Radiat. Environ. Biophys.* **43** 165-171

Ballarini F and Ottolenghi A 2005 A model of chromosome aberration induction: applications to space research *Radiat. Res.* **164** 567–70

Battistoni G, Bauer J, Boehlen TT, Cerutti F, Chin MPW, Dos Santos Augusto R, Ferrari A, Ortega PG, Kozłowska W, Magro G, Mairani A, Parodi K, Sala PR, Schoofs P, Tessonnier T and Vlachoudis V 2016 The FLUKA Code: An Accurate Simulation Tool for Particle Therapy *Front. Oncol.* **6** 116

Belli M, Cera F, Cherubini R, Dalla Vecchia M, Haque AMI, Ianzini F *et al* 1998 RBE-LET relationship for cell inactivation and mutation induced by low energy protons in V79 cells: further results at the LNL facility *Int. J. Radiat. Biol.* **74** 501-509

Campa A, Alloni D, Antonelli F, Ballarini F, Belli M, Dini V, Esposito G, Facoetti A, Friedland W, Furusawa Y, Liotta M, Ottolenghi A, Paretzke HG, Simone G, Sorrentino E and Tabocchini MA 2009 DNA fragmentation induced in human fibroblasts by 56Fe ions: experimental data and MC simulations *Radiat. Res.* **171** 438-445

Carabe-Fernandez A, Moteabbed M, Depauw N, Schuemann J and Paganetti H 2012 Range uncertainty in proton therapy due to variable biological effectiveness *Phys. Med. Biol.* **57** 1159-1172

Carante MP, Altieri S, Bortolussi S, Postuma I, Protti N and Ballarini F 2015 Modelling radiation-induced cell death: role of different levels of DNA damage clustering *Radiat. Environ. Biophys.* **54** 305–316

Carante MP and Ballarini F 2017 Modelling cell death for cancer hadrontherapy *AIMS Biophys.* **4** 465-490

Carante MP and Ballarini F 2016 Calculating Variations in Biological Effectiveness for a 62 MeV Proton Beam *Front. Oncol.* **6** 76

Carrano AV 1973 Chromosome aberrations and radiation-induced cell death. I. Transmission and survival parameters of aberrations *Mutat. Res.* **17** 341-353

Chatterjee A and Schaefer HJ 1976 Microdosimetric structure of heavy ion tracks in tissue *Radiat. Environ. Biophys.* **13** 215-227

Chaudhary P, Marshall T, Perozziello FM, Manti L, Currell FJ, Hanton F, McMahon SJ, Kavanagh JN, Cirrone GAP, Romano F, Prise KM and Schettino G 2014 Relative Biological Effectiveness Variation Along Monoenergetic and Modulated Bragg Peaks of a 62-MeV Therapeutic Proton Beam: Preclinical Assessment *Int. J. Radiat. Oncol. Biol. Phys.* **90** 27-35

Cornforth MN, Bedford JS 1985 On the Nature of a Defect in Cells from Individuals with Ataxia-Telangiectasia *Science* **227** 1589-1591

Cornforth M and Bedford J 1987 A quantitative comparison of potentially lethal damage repair and the rejoining of interphase chromosome breaks in low passage normal human fibroblasts *Radiat. Res.* **111** 385-405

Cremer C, Muenkel Ch, Granzow M, Jauch A, Dietzel S, Eils R, Guan X-Y, Meltzer PS, Trent JM, Langowski J and Cremer T 1996 Nuclear architecture and the induction of chromosomal aberrations *Mutat. Res.* **366** 97-116

Cuttone G, Cirrone GAP, Di Franco G, La Monaca V, Lo Nigro S, Ott J *et al* 2011 CATANA protontherapy facility: The state of art of clinical and dosimetric experience *Eur. Phys. J. Plus* **126** 65

Folkard M, Prise KM, Vojnovic B, Newman HC, Roper MJ and Michael BD 1996 Inactivation of V79 cells by low-energy protons, deuterons and helium-3 ions *Int. J. Radiat. Biol.* **69** 729-738

Furusawa Y, Fukutsu K, Aoki M, Itsukaichi H, Eguchi-Kasai K, Ohara H, Yatagai F, Kanai T and Ando K 2000 Inactivation of Aerobic and Hypoxic Cells from Three Different Cell Lines by

Accelerated ^{3}He-, ^{12}C- and ^{20}Ne-Ion Beams *Radiat. Res.* **154** 485-496

Grün R, Friedrich T, Krämer M and Scholz M 2017 Systematics of relative biological effectiveness measurements for proton radiation along the spread out Bragg peak: experimental validation of the local effect model *Phys. Med. Biol*. **62** 890-908

Hamada N, Funayama T, Wada S, Sakashita T, Kakizaki T, Ni M and Kobayashi Y 2006 LET-dependent survival of irradiated normal human fibroblasts and their descendents *Radiat. Res.* **166** 24-30

Kase Y, Kanai T, Matsumoto Y, Furusawa Y, Okamoto H, Asaba T, Sakama M and Shinoda H 2006 Microdosimetric measurements and estimation of human cell survival for heavy-ion beams *Radiat. Res.* **166** 629–38

Kavanagh JN, Currell FJ, Timson DJ, Savage KI, Richard DJ, McMahon SJ, Hartley O, Cirrone GAP, Romano F, Prise KM, Bassler N, Holzscheiter MH and Schettino G 2013 Antiproton induced DNA damage: proton like in flight, carbon-ion like near rest *Scientific Rep.* **3** 1770

Kiefer J and Straaten H 1986 A model of ion track structure based on classical collision dynamics *Phys. Med. Biol.* **31** 1201–9

Mairani A, Dokic I, Magro G, Tessonnier T, Kamp F, Carlson DJ, Ciocca M, Cerutti F, Sala PR, Ferrari A, Böhlen TT, Jäkel O, Parodi K, Debus J, Abdollahi A and Haberer T 2016 Biologically optimized helium ion plans: calculation approach and its *in vitro* validation *Phys. Med. Biol.* **61** 42-83-4299

Marshall TI, Chaudhary P, Michaelidesová A, Vachelová J, Davídková M, Vondráček V, Schettino G and Prise KM 2016 Investigating the implications of a variable RBE on proton dose fractionation across a clinical pencil beam scanned spread-out Bragg peak *Int. J. Radiat. Oncol. Biol. Phys.* **95** 70-77

McNamara AL, Schuemann J, Paganetti H 2015 A phenomenological relative biological effectiveness (RBE) model for proton therapy based on all published in vitro cell survival data *Phys. Med. Biol.* **60** 8399-8416

Michaelidesová A, Vachelová J, Puchalska M, Brabcová KP, Vondráček V, Sihver L, Davídková M 2017 Relative biological effectiveness in a proton spread-out Bragg peak formed by pencil beam scanning mode *Australas. Phys. Eng. Sci. Med.* **40** 359-368

Neti PVSV, de Toledo SM, Perumal V, Azzam EI and Howell RW 2004 A Multi-port Low-Fluence Alpha-Particle Irradiator: Fabrication, Testing and Benchmark Radiobiological Studies *Radiat. Res.* **161** 732-738

Ottolenghi A, Ballarini F and Merzagora M 1999 Modelling radiation-induced biological lesions: From initial energy depositions to chromosome aberrations *Radiat. Environ. Biophys.* **38** 1–13

Ottolenghi A, Ballarini F and Biaggi M 2001 Modelling chromosomal aberration induction by ionising radiation: the influence of interphase chromosome architecture *Adv. Space Res.* **27** 369-382

Paganetti H *et al* 2002 Relative Biological Effectiveness (RBE) values for proton beam therapy *Int. J. Radiat. Oncol. Biol. Phys.* **53** 407–421

Paganetti H and van Luijk P 2013 Biological considerations when comparing proton therapy and photon therapy *Semin. Radiat. Oncol.* **23** 77–87

Sato T, Niita K, Matsuda N, Hashimoto S, Iwamoto Y, Noda S, Iwase H, Nakashima H, Fukahori T, Chiba S and Sihver L 2014 Overview of the PHITS code and its application to medical physics *Prog. Nucl. Sci. Technol.* **4** 879-882

Schipler A and Iliakis G 2013 DNA double-strand-break complexity levels and their possible contributions to the probability for error-prone processing and repair pathway choice *Nuc. Acids Res.* **41** 7589-7605

Scholz M and Kraft G 1994 Calculation of Heavy Ion Inactivation Probabilities Based on Track Structure, X Ray Sensitivity and Target Size *Radiat. Prot. Dosim*. **52** 29-3

Tello JJ, Carante MP, Bernal M and Ballarini F 2017 Proximity effects in chromosome aberration induction by low-LET ionizing radiation *DNA Repair* **58** 38–46

Tello JJ, Carante MP, Bernal M and Ballarini F 2018 Proximity effects in chromosome aberration induction: dependence on radiation quality, cell type and dose *DNA Repair* accepted

Testa A, Ballarini F, Giesen U, Monteiro Gil O, Carante MP, Langner F, Rabus H, Palma V, Pinto M and Patrono C 2018 Analysis of radiation-induced chromosomal aberrations on cell-by-cell basis after 4He-ion microbeam irradiation: experimental data and simulations *Radiat. Res.* accepted

Tilly N, Johansson J, Isacsson U, Medin J, Blomquist E, Grusell E and Glimelius B 2005 The influence of RBE variations in clinical proton treatment plan for a hypopharynx cancer *Phys. Med. Biol.* **50** 2765-77

Tommasino F, Scifoni E and Durante M 2015 New ions for therapy *Int. J. Particle Ther.* **2** 428–438

Wedenberg M, Lind BK and Hardemark B 2013 A model for the relative biological effectiveness of protons: the tissue specific parameter α/β of photons is a predictor for the sensitivity to LET changes *Acta Oncol.* **52** 580-588

Wu H, George K and Yang TC 1999 Estimate of the frequency of true incomplete exchanges in human lymphocytes exposed to 1 GeV/u Fe ions in vitro *Int. J. Radiat. Biol.* **75** 593-599

Wu H, Furusawa Y, George K, Kawata T and Cucinotta FA 2002 Analysis of unrejoined chromosomal breakage in human fibroblast cells exposed to low- and high-LET radiation *J. Radiat. Res.* **43** S181-5